Further polarization measurements at 75 cm

Brouw, W.N.; Muller, C.A.; Tinbergen, J.

FURTHER POLARIZATION MEASUREMENTS AT 75 CM

BY W. N. BROUW, C. A. MULLER AND J. TINBERGEN

This paper reports a new series of polarization observations at 408 Mc/s made with a phase-switching receiver in conjunction with the 25-metre radio telescope at Dwingeloo. The detection of "spurious polarized radiation" and the removal of its effect on the observations are discussed, and possible sources indicated. Faraday rotation in the ionosphere is used as a proof of the existence of polarized radiation from outside the atmosphere, although the ionospheric dato are too doubtful to allow a correction. The area of intense polarization near $l^{II} = 140°$, $b^{II} = +5°$ is mapped in greater detail and its probable extent is determined.

1. *Introduction*

After the apparently successful measurement of a polarized component in the galactic 75 cm radiation reported by WESTERHOUT *et al.* (1962, hereafter referred to as paper 1), one of the present authors (C.A.M.) designed a new receiver based on the same correlation principle. The present paper gives the results of measurements made with this new instrument between September 25 and October 23, 1961.

There were three main purposes in the investigation. In the first place the detection of the ionospheric Faraday rotation, since this forms the best proof of the existence of polarized radiation from outside the earth's atmosphere; secondly an estimate of the various errors affecting the measurements; and thirdly more detailed mapping of the area of intense polarization near $l^{II} = 140°$, $b^{II} = +5°$.

As development of the equipment still continues, no detailed description of the instrument will be given and we shall limit ourselves to indicating the main differences between this instrument and that described in paper 1. The full advantages of a circular waveguide feed in reducing cross-polarization sidelobes of the antenna pattern of a parabolic reflector, as described in paper 1, were obtained by moving the dipole-probes further into the waveguide. An improved balun arrangement for feeding the dipole-probes reduced the coupling between the probes to better than 50 db. This led to more balanced excitation of the probes, and better suppression of the TEM mode in the (coaxial) circular waveguide feed.

The main differences between the present receiver and that described in paper 1 were the use of low-loss (0.25 db insertion loss) circulators between probes and receiver input, and the mounting of the entire front end close to the focus. A simpler design was chosen in which the hybrid network, add and subtract units, and one of the detectors were discarded. The changes in the feed arrangement and the use of a new receiver with circulators led to an improvement in stability and "instrumental zero error" of at least a factor five.

The telescope used was the 25-metre radio telescope of the Dwingeloo radio observatory. The centre frequency was 408 Mc/s, the bandwidth 1.7 Mc/s and the beamwidth 2°. The work was financially supported by the Netherlands Organization for the Advancement of Pure Research (Z.W.O.).

2. *Spurious polarized radiation*

After the first test measurements it was discovered that the result of a measurement at any point in the sky depended on the time at which the measurement was made. This suggested the existence of spurious polarized radiation varying with time, azimuth, or elevation, or any combination of these. Sweeps in azimuth and elevation showed that the main component varied systematically with elevation, while small systematic variations with azimuth and time were also present. Due to the rotation of the plane of polarization with time, and the fact that the sky polarization is irregular, the mean of a large number of sweeps in elevation made at various times and azimuths yields a good estimate of the systematic change of the spurious signal with elevation. There is some additional variation, which at present seems random; it could be due to man-made interference.

To facilitate the discussion of these effects, we shall use the Stokes parameters Q and U, which for linearly polarized radiation are

$$Q = \overline{T_b^p} \cos 2\theta$$
$$U = \overline{T_b^p} \sin 2\theta$$

where $\overline{T_b^p}$ and θ are the full-beam polarization brightness temperature and the polarization angle, respectively. Q and U are orthogonal components of the "polarization vector" used in paper 1. Q is the intensity measured when the probes make an angle of 45° with the direction $\theta = 0°$, while U is obtained when one of the probes is parallel to $\theta = 0°$.

Figure 1 shows, for Q and U (in the alt-azimuth system) separately, the results of individual sweeps taken on two different nights, and the mean of all the sweeps taken during the observing period. It is seen that there is indeed a systematic variation of the spurious signal with elevation, and that this consists mainly of changes in Q, corresponding to predominantly vertically polarized radiation (or horizontally polarized where Q is negative). There is also evidence that, at least for Q, there are systematic

FIGURE 1

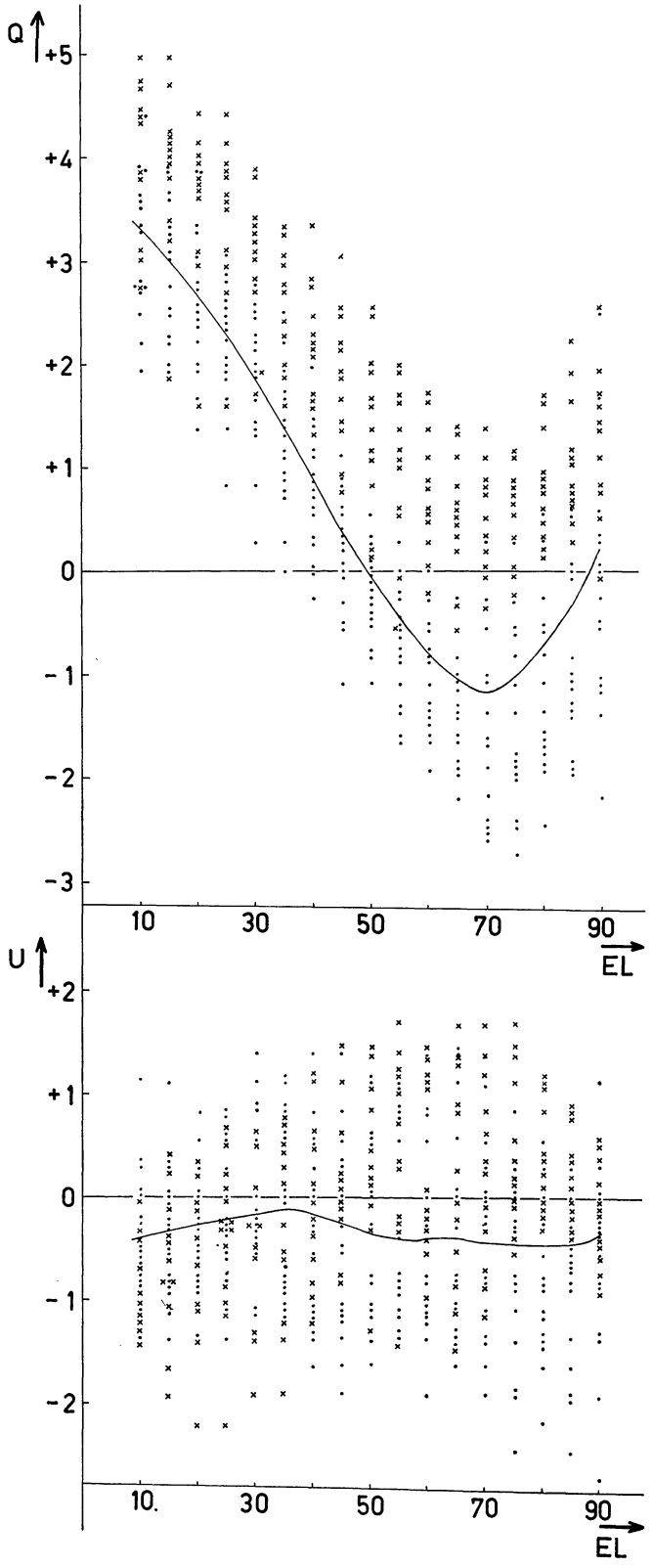

Variation of Q and U (°K) with elevation. Individual measurements for two nights, and mean of all measurements (full line).

differences between one night and another, approximately the same for all parts of the sky. This is borne out by analysis of the calibration measurements at three standard points in the sky, as discussed in section 3.

In addition to the sweeps in elevation, some sweeps were made in azimuth, at several elevations. After subtraction of the mean spurious signal for each elevation, there was still some systematic variation of the signal with azimuth (see Figure 2). Though we suspect that this variation is not the same at all elevations, we have not enough material to test this effectively.

Sweeps in elevation, made on successive nights, at the same azimuth and the same sidereal time, show some apparently random differences. Since the sky background must be the same for these observations, the variability must originate in the spurious radiation. This fact introduces uncertainties in the corrections to be applied to the observations, and largely determines the accuracy of our final results.

Though we have this empirical evidence for the existence of the "spurious polarized radiation", its source is still uncertain. In the first place, we cannot distinguish between an "instrumental zero error" (see paper 1) and a signal entering the equipment from the outside, although it is to be noted that the zero error is probably small. On the other hand, no single mechanism which could produce apparently polarized radiation varying with elevation seems sufficient to explain the observations. There are at least three mechanisms which could contribute to this spurious radiation. Radiation, from the sky near the horizon, and from the earth, travelling along the surface of the earth might become partly vertically polarized. Sky radiation reflected from the ground

FIGURE 2

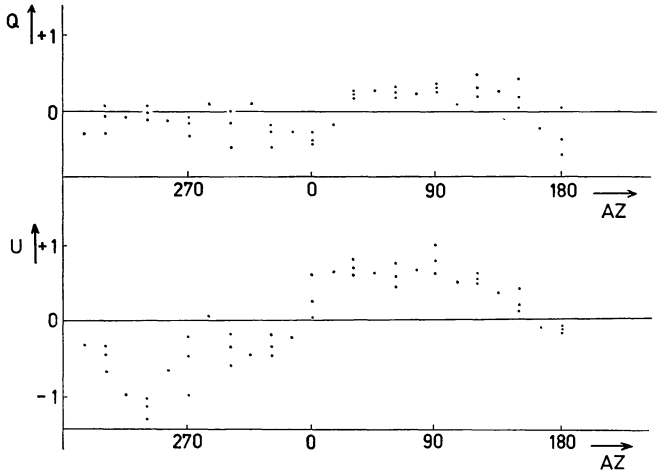

Variation of Q and U (°K) with azimuth after subtraction of component dependent on elevation.

will be partly horizontally polarized. Lastly, radiation in the spillover sidelobes will, in travelling past the edge of the mirror, become partly polarized at right angles to this edge.

The fact that, with the main beam at zero elevation, we measure vertically polarized radiation with $\overline{T_b^p} = 15$ °K indicates that at least the first mechanism is active.

Since the Dwingeloo telescope is surrounded on the one side by open heathland and on the other by pinewoods, it is not surprising that a small systematic variation with azimuth exists.

3. *Observations*

From the previous section it can be seen that, even though we can largely correct for the systematic variations of the spurious polarization, our estimate of the corrections will not be perfect, and small errors may remain. These errors are systematic when referred to the alt-azimuth coordinate system, but, by observing each point in the sky at several different times, we may change them into random errors in the final result. Accordingly, we tried to obtain at least two such independent observations at each point.

The intensities and polarization angles were determined by means of an overlay of standard sine curves (see paper 1). The quantities Q and U for the alt-azimuth system were formed, and corrected for the elevation- and azimuth-dependent parts of the spurious radiation.

If the spurious radiation would vary with elevation and azimuth only, then, for one position in the sky, the corrected values of Q and U should define a circle in the Q-U plane, with its centre at the origin (see paper 1, Figure 5). To evaluate a possible variation of the spurious radiation with time, measurements at the position $l^{II} = 141°$, $b^{II} = +8°$ were used. This point was observed 10 to 20 times each night for calibration purposes. Least-squares solutions to determine the centre of the circle for each night showed that the position of this centre changed from one night to another. During two nights two other points were observed as often as the calibration point. Results of least-squares solutions for all three points during these nights are shown in Table 1.

TABLE 1

Coordinates of the centres of the circles swept out by the polarization vectors for three points, on two nights.

Date	b^{II}	l^{II}	Q_o	m.e.	U_o	m.e.	Elevation
14/15 Oct.	+ 8°	141°	+0.5°K	±0.2	+0.9°K	±0.2	40°–80°
	+27	123	+0.6	0.1	+0.8	0.1	53
	+57	116	+0.5	0.1	+0.3	0.2	20–40
15/16 Oct.	+ 8	141	+1.4	0.2	+0.6	0.2	40–80
	+27	123	+1.3	0.1	+0.7	0.1	53
	+57	116	+1.3	0.1	+0.5	0.1	20–40

It can be seen that for each night the Q and U coordinates of the centres of the three circles were the same, although the elevations at which the observations were made differed widely. Taken with the evidence of Figure 1, this strongly suggests the existence in the spurious radiation of a component varying from night to night, but independent of position in the sky. The observations at the calibration point allow a correction to be derived for each night.

A search was made for components of the spurious radiation which varied systematically with the time of night, or with the temperature of the first stage of the receiver, but in both cases no statistically significant effects were found.

After correction for all the systematic effects discussed above, the values of Q and U relative to the galactic coordinate system were calculated, and averaged for each position in the sky. From these mean values the full-beam polarization brightness temperature $\overline{T_b^p}$ and the galactic polarization angle θ_{gal} were calculated.

The results are shown in Figure 3 and Table 2. The length and direction of the lines indicate $\overline{T_b^p}$ and θ_{gal}. Dots were plotted where the intensity was 0.8 °K or less. A dot superposed on a line indicates that only one measurement was made at that position, and that the result is uncertain.

Figure 3 shows that the limits of the area of intense polarization near $l^{II} = 140°$, $b^{II} = +5°$ are now fairly well known. The region seems to be unusually large (400 square degrees) and bright; rough measurements in some other parts of the sky have failed to uncover similar bright areas.

The internal mean error for a single measurement is 0.6 °K in $\overline{T_b^p}$, and $\frac{17}{\overline{T_b^p}}$ degrees in θ_{gal}. The error distribution is perfectly Gaussian.

It is difficult to give a reliable estimate of systematic errors. Now that the results begin to have a generally plausible appearance, one might be tempted to think that remaining systematic errors must be small. At the present early stage this is dangerous. We

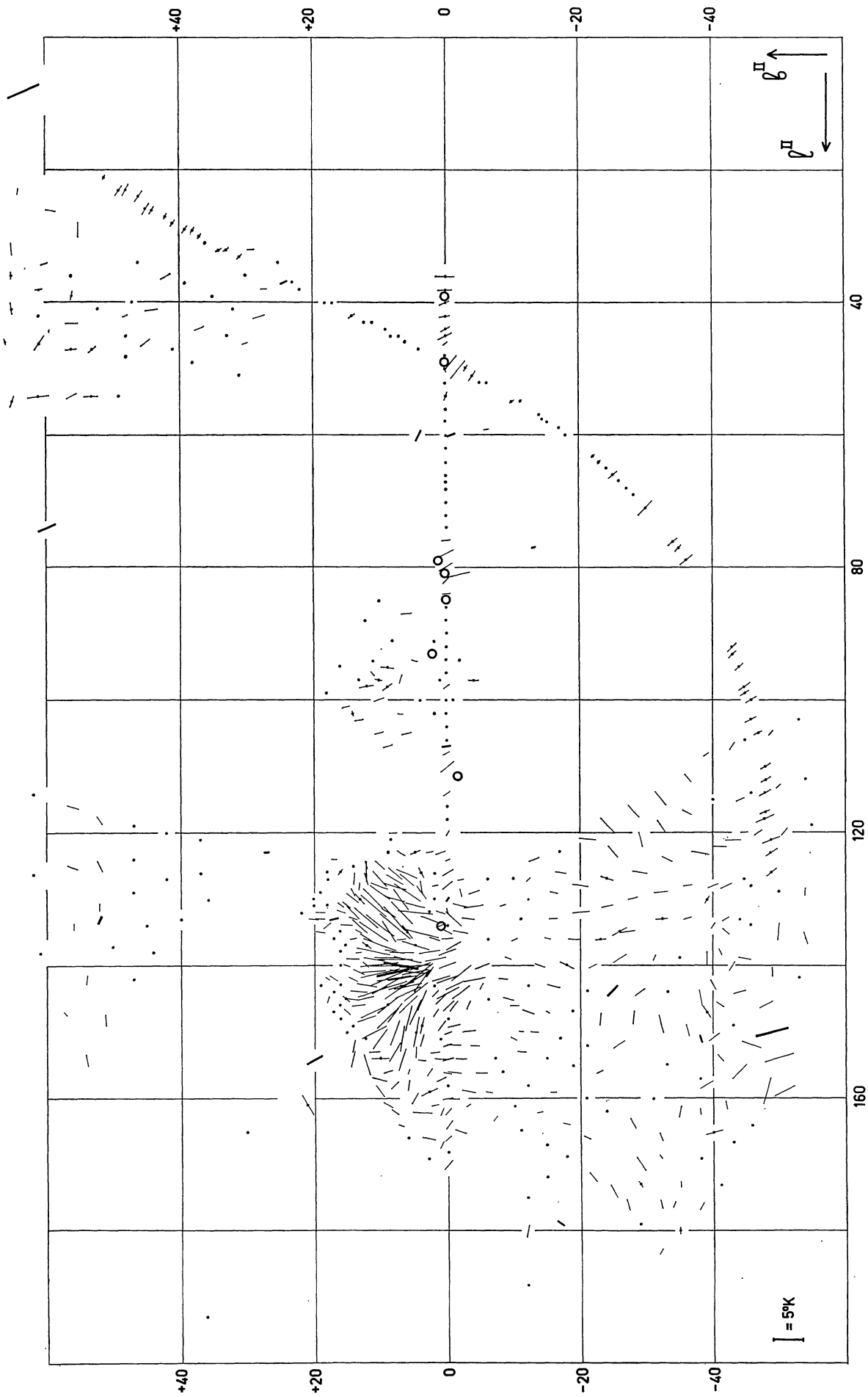

FIGURE 3

Polarization measurements at 75 cm. The length and direction of the lines indicate $\overline{T_b^p}$ and θ_{gal}. Thick lines refer to measurements made five times or more, thin lines two, three or four times, and lines with superimposed dots once. Dots denote $\overline{T_b^p} < 0.8$ °K. Circles give the positions of point sources which might have influenced measurements within 3°. No correction for ionospheric Faraday rotation was applied.

know, for instance, that there is a systematic error in the polarization angles due to ionospheric Faraday rotation (see section 4), but this cannot be deduced from the appearance of Figure 3. There may be other, unsuspected, sources of systematic error.

The systematic error in θ_{gal} due to ionospheric Faraday rotation was calculated for a parabolic F layer. We used the f_0F_2 and y_mF_2 measured at De Bilt and a value of $H\cos\Phi\sec z$ averaged approximately for the directions in which we observed. On this basis the systematic error in θ_{gal} is $+8$ degrees. The actual systematic error is probably between 2 and 4 times as large (see section 4).

TABLE 2

Full-beam polarization brightness temperature and position angle (uncorrected for ionospheric Faraday rotation) with respect to the galactic North pole of the polarized radiation at 75 cm.

b^{II}	l^{II}	$\alpha_{1950.0}$	$\delta_{1950.0}$	$\overline{T_b^p}$	θ_{gal}	n	b^{II}	l^{II}	$\alpha_{1950.0}$	$\delta_{1950.0}$	$\overline{T_b^p}$	θ_{gal}	n
−55°	119°	10°	8°	0.4 °K	99°	2	−44°	95°	352°	14°	1.8 °K	51°	1
								115	6	18	1.3	31	2
−54	112	6	8	0.8	103	2		133	20	18	0.4	144	2
	129	16	8	1.5	91	2		144	28	16	1.9	21	2
	136	20	8	2.4	124	2		156	36	12	3.2	52	2
−53	103	0	8	0.3	55	2	−43	92	349	14	1.8	54	1
	142	24	8	0.3	157	2		93	350	14	1.8	53	1
								107	0	18	1.3	60	2
−51	120	10	12	1.5	57	2		121	11	20	2.5	7	1
	159	28	8	3.8	33	2		140	25	18	1.6	153	2
								149	32	16	0.3	174	2
−50	113	6	12	1.0	51	2		169	44	8	0.1	50	2
	129	16	12	0.7	126	2							
	135	20	12	2.7	90	2	−42	128	16	20	1.8	33	2
	154	32	8	5.2	23	4		133	20	20	1.2	37	2
								135	22	20	1.4	145	1
−49	105	0	12	1.0	56	2		161	40	12	1.3	107	2
	121	11	14	3.1	27	1							
	123	12	14	2.3	39	1	−41	122	11	22	2.5	4	1
	126	14	14	2.1	45	1		138	24	20	1.0	121	2
	141	24	12	1.6	96	2		146	30	18	1.6	152	2
	150	30	9.5	5.8	21	6		154	36	16	1.4	138	2
								173	48	8	0.5	10	3
−48	110	3	14	1.8	38	1							
	112	5	14	1.8	36	1	−40	115	6	22	0.6	164	2
	114	6	14	2.1	36	1		128	16	22	1.6	27	2
	117	8	14	1.8	32	1		134	21	22	1.2	61	2
	118	9	14	3.2	30	1		143	28	20	2.1	124	2
	146	28	12	2.5	33	2		151	35	18	2.2	43	2
	159	36	8	4.4	80	2		165	44	12	2.7	20	1
−47	105	0	14	1.4	36	1	−39	108	0	22	1.1	39	2
	120	10	16	1.6	43	2		130	18	23	1.3	61	1
								139	26	22	2.5	96	2
−46	100	356	14	2.0	37	1		147	32	20	2.5	129	1
	103	358	14	2.0	34	1		158	40	16	2.5	38	2
	114	6	16	0.6	79	2							
	128	16	16	0.8	40	2	−38	169	48	12	0.7	17	3
	134	20	16	0.5	0	2		176	52	8	1.5	69	2
	152	32	12	3.4	166	2							
	164	40	8	0.7	2	2	−37	123	12	26	2.8	175	2
								145	31	22	3.0	107	2
−45	98	354	14	2.3	41	1		151	36	20	1.3	114	11
	99	355	14	1.4	42	1		157	40	18	0.6	160	2
	106	0	16	0.6	110	2		162	44	16	1.1	106	2
	120	10	18	1.0	13	2							
	127	15	18	0.7	141	2	−36	79	337	14	2.6	44	1
	139	24	16	2.3	177	2		112	2	26	1.4	135	2

TABLE 2 *(continued)*

b^{II}	l^{II}	$\alpha_{1950.0}$	$\delta_{1950.0}$	$\overline{T_b^p}$	θ_{gal}	n	b^{II}	l^{II}	$\alpha_{1950.0}$	$\delta_{1950.0}$	$\overline{T_b^p}$	θ_{gal}	n
−36°	117°	7°	26°	1.7 °K	158°	2	−23°	64°	317°	14°	1.0 °K	59°	1
	128	17	26	1.5	16	2		136	27	38	1.8	9	1
	134	22	26	1.2	26	2		148	40	34	2.0	91	2
	150	36	22	2.0	110	2		156	48	30	0.8	31	2
−35	77	335	14	1.6	53	1	−22	63	316	14	1.0	46	1
	139	27	26	0.3	173	2		140	32	38	1.3	33	2
	162	45	18	1.9	86	2		172	61	22	2.0	136	2
	173	52	12	0.9	97	2							
	180	56	8	1.3	95	1	−21	121	10	42	2.7	1	2
								124	14	42	1.3	68	2
−34	76	334	14	1.9	44	1		144	37	38	0.6	1	2
	166	48	16	1.1	166	2		152	45	34	0.4	17	2
								160	53	30	0.8	0	2
−33	124	13	30	1.8	160	2		166	57	26	1.0	163	2
	144	32	26	0.7	60	2							
	155	41	22	0.6	115	2	−20	128	19	42	2.6	177	2
								132	24	42	2.7	10	2
−32	115	4	30	2.9	134	2							
	119	8	30	2.3	130	2	−19	136	29	42	1.8	1	2
	129	18	30	2.2	11	2		147	42	38	0.6	61	2
	134	23	30	2.0	12	1		155	50	34	0.6	18	2
	149	37	26	3.3	110	2							
	166	50	18	1.6	117	2	−18	60	311	14	1.0	49	1
	169	52	16	1.0	133	2		140	34	42	2.5	160	1
	176	56	12	1.5	109	2		164	58	30	1.1	174	2
	183	60	8	1.1	66	2		169	62	26	0.4	142	2
−31	139	28	30	1.1	72	2	−17	59	310	14	0.7	57	1
	160	46	22	0.5	21	2		123	12	46	0.7	163	2
								126	16	46	1.7	177	2
−30	71	327	14	3.2	52	1		151	47	38	0.6	137	2
								179	70	20	1.3	150	29
−29	121	10	34	2.6	111	2							
	126	15	34	2.3	177	2	−16	129	21	46	1.1	174	2
	144	33	30	1.9	43	2		133	26	46	1.2	8	2
	170	55	18	2.5	129	2		143	39	42	2.0	171	2
	173	56	16	1.1	128	1		159	55	34	0.9	4	2
	179	60	12	0.7	86	2							
							−15	58	308	14	0.7	48	1
−28	69	325	14	0.8	63	1		136	31	46	1.0	173	2
	117	6	34	2.9	139	2		147	44	42	0.8	154	2
	130	20	34	1.5	19	4		154	52	38	0.4	166	2
	148	38	30	2.2	92	1		167	63	30	0.6	15	2
	164	51	22	2.0	123	2		172	67	26	0.3	167	2
−27	68	323	14	0.7	64	1	−14	57	306	14	1.0	51	1
	135	25	34	2.4	13	2		58	307	14	0.7	48	1
	176	60	16	2.0	111	2		140	36	46	1.6	165	2
								162	60	34	0.7	21	2
−26	67	322	14	0.8	64	1							
	135	30	34	2.8	34	1							
	139	30	34	2.4	39	2	−13	77	318	30	0.6	18	53
	152	43	30	2.2	39	2		124	14	50	2.1	28	2
								150	49	42	1.2	2	2
−25	66	320	14	1.7	44	1							
	123	12	38	2.5	135	2							
	144	35	34	2.5	52	5	−12	127	18	50	1.0	51	2
	174	60	18	2.5	125	2		130	23	50	0.3	140	2
								143	41	46	1.1	3	2
−24	65	319	14	0.7	67	1		147	46	44	2.1	169	2
	119	8	38	3.3	140	2		158	57	38	3.4	175	2
	127	17	38	2.2	168	1		175	72	26	3.9	120	2
	131	22	38	1.6	19	2		180	75	22.1	1.9	86	2
	162	52	26	1.1	166	2		188	79	15.5	0.9	6	4

TABLE 2 *(continued)*

b^{II}	l^{II}	$\alpha_{1950.0}$	$\delta_{1950.0}$	$\overline{T_b^p}$	θ_{gal}	n	b^{II}	l^{II}	$\alpha_{1950.0}$	$\delta_{1950.0}$	$\overline{T_b^p}$	θ_{gal}	n
−11°	55°	303°	14°	1.0 °K	60°	1	−1°	100°	330°	54°	0.3 °K	89°	2
	133	28	50	0.6	71	2		133	32	60	3.4	143	2
	150	50	44	0.9	175	2		137	40	58	2.5	38	2
	153	54	42	1.3	179	2		143	50	56	3.3	31	2
	165	65	34	0.4	29	2		146	54	54	2.0	57	2
								149	58	52	1.9	21	2
−10	55	302	14	1.1	44	1		152	62	50	1.9	6	2
	127	19	52	0.8	31	1		156	66	48	2.2	179	2
	136	33	50	0.9	29	2		160	70	44	1.4	5	2
	146	46	46	1.3	5	2							
	151	52	44	1.1	159	2	0	36	283.6	2.7	3.3	6	1
	161	62	38	0.3	29	2		38	284.6	4.4	2.1	12	1
								40	285.5	6.2	1.7	29	1
−9	139	38	50	1.0	168	2		42	286.4	8.0	1.7	16	1
	145	46	48	1.5	170	2		44	287.4	9.8	1.5	38	1
								45	288.0	10.0	2.5	33	2
−8	131	26	54	1.0	20	2		46	288.3	11.6	1.0	46	1
	142	43	50	1.3	179	2		48	289.3	13.3	0.8	148	1
	156	59	42	0.7	6	2		50	290.3	15.0	1.0	106	1
								52	291.3	16.8	0.4	87	1
−7	154	58	44	0.6	5	2		54	292.3	18.6	1.5	79	1
	163	67	38	1.1	60	2		56	293.3	20.3	1.1	92	1
								58	294.4	22.0	0.8	98	1
−6	52	297	14	0.4	39	1		60	295.5	23.8	0.3	33	2
	59	300	20	1.0	14	1		62	296.6	25.5	0.2	21	2
	127	20	56	0.8	163	2		64	297.7	27.2	0.5	90	2
	136	34	54	0.6	24	2		66	298.9	28.9	0.8	34	2
	145	48	50	0.5	70	3		67	300.0	30.0	0.8	20	1
	159	64	42	0.9	0	2		68	300.1	30.6	0.7	34	2
								70	301.4	32.3	0.4	39	2
−5	52	296	14	0.7	68	1		72	302.7	34.0	0.4	64	1
	140	42	54	2.2	24	2		74	304.1	35.6	0.6	47	2
	143	46	52	1.1	68	2		76	305.5	37.3	1.5	12	2
	156	62	44	1.6	2	2		78	307.0	38.9	2.9	34	2
								80	308.5	40.5	2.7	37	2
−4	51	294	14	1.9	62	1		82	310.2	42.1	1.5	50	2
	97	330	50	1.3	8	1		84	311.9	43.7	1.3	11	2
	129	24	58	1.8	24	2		86	313.7	45.2	0.6	140	2
	131	28	58	3.0	14	2		88	315.6	46.7	0.0	—	2
	142	46	54	3.3	18	2		90	317.6	48.1	0.2	41	2
	152	58	48	1.2	5	2		92	319.7	49.6	0.9	54	2
								94	322.0	50.9	0.8	61	2
−3	50	293	14	1.5	66	1		96	324.3	52.3	0.7	45	2
	133	32	58	1.8	179	2		98	326.9	53.6	1.0	44	2
	146	52	52	1.7	72	2		100	329.6	54.8	0.6	71	2
	150	58	50	2.2	7	2		102	332.4	56.0	0.1	61	2
	159	66	44	2.2	175	2		104	335.5	57.1	0.5	103	2
	161	69	42	0.9	38	2		106	338.7	58.1	0.5	50	2
								107	340.0	59.0	1.3	16	8
−2	50	292	14	3.8	157	2		108	342.0	59.0	1.2	33	2
	81	312	40	3.2	18	2		110	345.6	59.9	2.9	45	2
	94	324	50	0.5	177	1		114	353.3	61.3	1.0	128	2
	127	20	60	0.8	13	2		116	357.3	61.8	0.4	80	2
	129	24	60	1.2	108	2		118	1.5	62.2	0.3	76	2
	131	28	60	2.6	170	2		120	5.8	62.5	1.0	67	2
	135	36	58	2.3	174	2		122	10.1	62.6	0.5	19	2
	141	46	56	3.8	43	2		124	14.4	62.6	1.1	30	2
	144	50	54	3.2	42	2		126	18.8	62.5	2.0	36	2
	154	62	48	1.6	4	2		128	23.0	62.2	2.0	45	4
	165	74	40	1.7	77	3		130	27.2	61.8	0.9	58	7
								132	31.2	61.3	1.0	113	2
−1	49	291	14	2.7	59	2		134	35.2	60.6	0.7	136	2
	60	296	23	1.3	28	7		135	36.0	60.0	1.5	160	2

TABLE 2 *(continued)*

b^{II}	l^{II}	$\alpha_{1950.0}$	$\delta_{1950.0}$	$\overline{T_b^p}$	θ_{gal}	n	b^{II}	l^{II}	$\alpha_{1950.0}$	$\delta_{1950.0}$	$\overline{T_b^p}$	θ_{gal}	n
0°	136°	38.9°	59.9°	2.0 °K	9°	4	+4°	141°	51°	61°	4.8 °K	44°	4
	138	42.5	59.0	2.8	27	2		142	54	60	4.5	60	2
	140	45.9	58.1	2.9	24	3		145	58	58	4.1	71	2
	142	49.1	57.1	3.8	27	2		149	64	56	2.8	82	1
	144	52.1	56.0	4.2	32	2		151	66	54	2.4	80	2
	146	54.9	54.8	2.5	49	2		154	70	52	1.1	178	2
	148	57.6	53.6	1.0	82	4		162	78	46	3.1	83	3
	150	60.2	52.3	1.1	29	2							
	152	62.6	50.9	1.5	23	2	+5	94	316	54	0.9	173	2
	154	64.8	49.6	2.0	19	2		123	12	68	1.7	29	1
	156	66.9	48.1	1.4	179	2		131	32	66	3.3	172	2
	158	69.0	46.7	0.2	25	2		132	36	66	6.0	178	2
	160	70.8	45.2	1.3	13	2		137	46	64	4.8	167	1
	162	72.6	43.6	1.5	53	2		140	51	62.5	4.9	8	3
	164	74.4	42.1	1.8	58	2		141	54	62	4.6	17	2
	166	76.0	40.5	1.3	49	2		142	54	61	5.7	37	3
	168	77.5	38.9	0.4	71	2		144	58	60	5.0	43	2
	170	79.0	37.0	2.0	54	2		147	62	58	4.7	69	2
								150	66	56	5.0	85	1
+1	97	324	54	0.7	59	2		153	70	54	1.6	93	2
	123	12	64	1.6	22	2		160	78	48	2.0	67	2
	132	32	62	1.4	165	3							
	134	36	62	1.5	25	3	+6	46	283	14	0.2	170	1
	142	50	58	3.1	23	2		87	308	50	1.7	11	2
	145	54	56	2.7	49	2		105	330	62	1.5	21	2
	149	60	54	2.1	58	2		126	20	68	3.6	161	2
	151	62	52	0.8	6	2		127	24	68	2.8	146	2
	154	66	50	2.2	1	2		129	28	68	5.0	151	2
	157	70	48	1.6	33	3		135	42	66	2.8	133	1
	162	74	44	1.5	74	3		139	50	64	4.5	172	6
	167	78	40	1.3	67	3		141	54	62.5	5.6	0	3
								143	58	62	4.6	18	6
+2	91	316	50	0.7	16	1		144	60	61	4.6	31	3
	102	330	58	1.0	179	1		146	62	60	4.1	48	4
	126	20	64	0.6	59	2		148	66	58	4.5	80	2
	128	24	64	1.0	18	2		156	74	52	1.0	76	2
	130	28	64	0.4	175	2		158	76	50	2.0	86	2
	136	40	62	2.0	169	3		166	82	44	0.3	153	2
	139	46	60	3.3	15	2							
	143	52	58	0.6	170	2	+7	45	282	14	0.4	42	1
	144	54	58	1.7	53	4		97	316	58	1.5	77	2
	147	58	56	1.7	63	2		102	324	62	1.0	0	2
	153	66	52	1.6	13	2		123	12	70	1.5	152	2
	161	74	46	1.3	18	3		130	32	68	4.5	131	2
								132	36	68	5.2	140	2
+3	123	12	66	1.1	19	2		136	46	66	1.5	9	2
	132	32	64	0.4	133	2		138	51	65.5	4.0	4	3
	133	36	64	3.1	164	2		140	54	64	5.9	173	5
	138	46	62	3.4	15	2		142	57	62.5	5.1	16	3
	141	50	60	1.9	63	2		143	58	62	4.6	22	1
	156	70	50	1.5	62	2		151	70	56	4.5	86	4
	159	74	48	2.9	31	1		154	74	54	4.3	78	2
	164	78	44	2.0	83	3		164	82	46	1.0	169	2
	169	82	40	0.5	109	2							
							+8	45	280	14	1.0	58	1
+4	47	285	14	0.4	42	1		91	308	54	0.5	115	2
	60	192	26	2.1	71	60		120	4	70	1.1	10	2
	100	324	58	0.8	154	2		126	20	70	3.0	152	2
	126	20	66	2.0	121	1		127	24	70	3.1	156	4
	128	24	66	2.0	104	2		128	28	70	4.0	168	2
	129	28	66	2.6	132	2		130	32	70	3.4	170	2
	135	40	64	5.7	172	4		133	40	68	5.5	137	2
	140	50	62	3.6	25	2		134	44	68	6.5	146	2

TABLE 2 *(continued)*

b^{II}	l^{II}	$\alpha_{1950.0}$	$\delta_{1950.0}$	$\overline{T_b^p}$	θ_{gal}	n	b^{II}	l^{II}	$\alpha_{1950.0}$	$\delta_{1950.0}$	$\overline{T_b^p}$	θ_{gal}	n
+ 8°	138°	50°	66°	3.2 °K	177°	2	+12°	126°	24°	74°	3.1 °K	95°	2
	139	54	65.5	5.5	5	3		127	28	74	1.9	111	2
	141	57	64	5.5	8	299		133	46	72	5.1	145	4
	142	58	64	5.5	13	2		136	54	70	2.5	153	2
	143	60	62.5	4.6	23	3		137	56	70	1.7	149	1
	144	62	62	4.3	40	3		140	62	68	1.0	144	2
	147	66	60	4.1	57	2		143	66	66	3.4	175	4
	150	70	58	4.7	75	2		145	70	64	2.5	19	2
	153	74	56	3.8	64	2		148	74	62	3.1	24	2
	158	78	52	1.8	48	2		151	78	60	0.8	10	2
	162	82	48	1.4	153	2		155	82	56	3.6	113	2
+ 9	44	279	14	0.8	57	1	+13	97	308	62	0.2	104	2
	95	312	58	2.0	179	1		103	316	66	1.4	15	2
	98	316	60	2.0	41	1		128	32	75	1.3	91	2
	107	330	66	1.4	25	2		130	36	74	2.3	139	1
	123	12	72	0.1	28	2		134	50	72	3.3	143	2
	132	38	70	2.7	150	3		135	54	72	1.0	157	2
	135	46	68	4.2	128	2		138	58	70	1.0	10	2
	139	54	66	4.9	5	2		141	66	68	1.9	161	2
	140	57	65.5	6.6	6	3		144	70	66	2.9	1	2
	142	60	64	6.3	29	3		146	74	64	2.2	12	4
	143	62	64	5.5	34	2							
	146	66	62	4.2	44	1	+14	42	274	14	1.0	41	1
	148	70	60	4.8	51	2		92	300	58	1.0	109	1
	156	78	54	1.5	22	2		125	20	76	0.4	176	2
	161	82	50	1.7	156	2		127	28	76	2.1	92	2
								129	36	76	1.3	120	2
+10	85	300	50	0.8	32	2		130	40	75	2.4	148	2
	97	312	60	1.0	173	1		132	46	74	2.8	139	2
	100	316	62	1.7	25	2		133	50	74	1.3	169	2
	105	324	66	1.5	20	2		136	58	72	1.1	16	2
	125	20	72	2.3	145	2		139	62	70	2.1	5	2
	127	24	72	3.1	138	2		142	70	68	1.4	160	2
	128	28	72	3.0	164	2		145	74	66	2.1	177	2
	129	32	72	4.1	150	2		149	78	62	0.8	7	2
	134	44	70	5.9	147	3		152	82	60	2.1	86	2
	137	52	68	6.1	164	2		154	84	58	2.8	83	2
	140	58	66	6.3	12	2							
	141	60	65.5	6.9	17	3	+15	101	308	66	1.3	19	2
	151	74	58	4.3	59	2		131	44	76	1.7	147	2
	154	78	56	3.0	6	1		134	54	74	1.8	2	3
	157	80	54	2.2	169	2		137	62	72	0.6	25	2
	159	82	52	2.2	130	2		140	66	70	1.0	167	3
								145	76	66	1.4	144	1
+11	43	277	14	0.8	45	1		147	78	64	1.6	143	2
	94	308	58	0.5	153	2		150	82	62	0.1	56	2
	96	310	60	1.0	138	4							
	130	36	72	4.8	140	4	+16	95	300	62	0.4	34	2
	131	40	72	5.6	144	2		126	28	78	1.1	57	1
	135	50	70	5.6	151	3		131	46	76	1.2	149	2
	138	56	68	5.6	174	2		132	50	76	1.3	166	2
	139	58	68	3.6	176	2		135	58	74	0.4	151	2
	141	62	66	3.9	11	2		138	66	72	0.8	166	2
	144	66	64	5.2	23	2		140	70	70	0.8	134	1
	147	70	62	4.5	29	2		143	74	68	0.4	155	1
	150	74	60	4.5	32	2		146	78	66	0.8	123	2
	153	78	58	1.8	8	2		148	82	64	0.9	71	2
+12	43	276	14	0.8	45	1	+17	40	270	14	0.2	65	1
	88	300	54	0.8	179	2		124	20	80	1.0	0	3
	98	312	62	1.5	21	37		133	58	76	1.3	21	5
	125	20	74	0.9	108	2		136	66	74	0.7	36	3

TABLE 2 *(continued)*

b^{II}	l^{II}	$\alpha_{1950.0}$	$\delta_{1950.0}$	$\overline{T_b^p}$	θ_{gal}	n	b^{II}	l^{II}	$\alpha_{1950.0}$	$\delta_{1950.0}$	$\overline{T_b^p}$	θ_{gal}	n
+17°	142°	76°	70°	1.6 °K	153°	2	+37°	44°	252°	24°	1.5 °K	29°	2
	144	78	68	0.9	46	2		121	200	80	0.4	174	2
	147	82	66	0.7	72	2		126	180	80	0.5	50	2
+18	40	269	14	0.7	80	1	+38	29	246	14	1.0	64	1
	99	300	66	0.3	2	2		49	252	28	0.8	44	2
	126	28	80	0.8	167	3							
	127	36	80	0.3	101	3	+39	29	245	14	1.3	59	1
	131	50	78	0.5	2	4		37	248	20	0.1	162	2
	134	62	76	1.4	43	2							
	142	78	70	0.9	147	2	+40	42	248	24	1.2	40	2
	145	82	68	1.2	79	2		133	160	75	0.5	176	2
+19	129	44	80	0.7	62	3	+41	28	243	14	1.4	60	1
	132	58	78	1.4	5	2		47	248	28	0.3	93	2
	133	62	78	1.6	5	2							
	135	66	76	1.6	177	1	+42	27	242	14	1.0	67	1
	143	82	70	0.7	74	2		36	244	20	1.7	34	3
								120	200	75	0.6	32	2
+20	130	52	80	0.8	32	3		127	180	75	0.3	26	2
	131	60	80	0.4	176	2	+44	26	240	14	1.4	64	1
	133	66	78	1.4	1	2		41	244	24	2.0	14	3
	154	94	61	2.6	35	25		138	160	70	0.3	165	2
+21	161	100	55	3.8	156	1	+45	26	239	14	1.9	67	1
								46	244	28	1.8	43	3
+22	38	265	14	0.6	68	1							
	132	68	80	0.5	178	2	+46	24	237	14	2.1	60	1
								34	240	20	0.7	178	5
+23	37	263	14	0.8	58	1		134	170	70	0.4	125	2
+24	37	262	14	1.2	25	6	+47	40	240	24	0.7	167	5
								119	200	70	0.8	134	2
+25	34	260	12	0.8	157	2		124	190	70	0.2	37	2
								129	180	70	0.9	90	2
+27	38	260	16	1.0	7	2		142	160	65	0.5	99	2
	123	—	90	1.0	16	302							
							+48	23	235	14	1.9	66	1
+28	42	260	20	1.9	22	2		42	240	26	1.0	26	1
								45	240	28	0.7	6	5
+29	32	256	12	1.1	9	2		48	240	30	0.6	33	1
+30	36	256	16	0.7	28	2	+49	23	234	14	1.7	61	1
	46	260	24	1.0	23	2		54	240	34	0.3	95	1
	165	117	53	0.6	137	1							
							+50	137	170	65	0.3	89	2
+31	33	254	14	1.0	60	1							
	51	260	28	0.8	40	1	+51	21	232	14	1.0	65	1
								148	160	60	1.7	100	2
+32	41	256	20	0.8	3	2							
							+52	41	235	26	0.3	87	1
+33	32	252	14	1.0	42	1		118	200	65	1.4	130	2
	45	256	24	0.4	44	2		125	190	65	1.8	123	2
								131	180	65	1.2	98	2
+34	32	251	14	1.0	34	1		133	178	64	1.2	72	21
+35	39	252	20	0.7	49	2							
							+53	47	235	30	1.5	46	1
+36	31	249	14	0.8	48	1		54	235	34	2.2	5	1
	130	160	80	0.1	14	2							
	194	130	30	0.9	133	65							
							+54	142	170	60	1.4	91	3
+37	30	247	14	1.0	60	1		154	160	55	1.9	106	3

TABLE 2 *(continued)*

b^{II}	l^{II}	$\alpha_{1950.0}$	$\delta_{1950.0}$	$\overline{T_b^p}$	θ_{gal}	n	b^{II}	l^{II}	$\alpha_{1950.0}$	$\delta_{1950.0}$	$\overline{T_b^p}$	θ_{gal}	n
+55°	29°	230°	20°	2.3 °K	96°	2	+61°	42°	225°	28°	0.6 °K	57°	2
								46	225	30	2.8	61	1
+56	36	230	24	0.5	109	2		54	225	34	3.2	12	1
	39	230	26	1.8	80	1		138	180	55	0.6	3	4
	134	180	60	0.9	95	3							
							+62	114	200	55	0.8	24	3
+57	43	230	28	1.7	5	2		126	190	55	0.7	171	3
	47	230	30	1.6	9	1							
	54	230	34	1.9	33	1	+63	8	217	14	5.6	43	24
	116	200	60	1.5	168	48							
	125	190	60	1.5	163	3	+64	23	220	20	1.0	87	2
+58	147	170	55	0.9	139	3	+65	32	220	24	1.8	101	2
								36	220	26	0.9	94	1
+59	26	225	20	1.6	177	2		41	220	28	1.8	104	2
								55	220	34	1.7	78	1
+60	34	225	24	1.1	24	2							
	74	296	23	2.1	29	8	+66	46	220	30	1.0	114	1
+61	38	225	26	1.2	103	1	+71	128	190	46	0.7	102	14

4. *Ionospheric Faraday rotation*

The detection of ionospheric Faraday rotation forms the best, if not the only, proof that we observe polarized radiation from outside the earth's atmosphere. To use as large a range of rotations as possible, we made many observations at $l^{II} = 141°$, $b^{II} = +8°$ in the first few hours of the night, when the total electron content of the ionosphere changes rapidly. Similar measurements at some other points were made, but less frequently.

The Faraday rotation is given by (see paper 1)

$$\xi = \frac{e^3}{2\pi m^2 f^2 c^2} \int_{\text{ray path}} N . H . \cos\Phi . \sec z . dh \text{ radians.}$$

Mr R. S. ROGER, of the Nuffield Radio Astronomy Laboratories at Jodrell Bank, has kindly provided us with a table of values of the function $H . \cos\Phi . \sec z$, computed for Dwingeloo, for a sheath ionosphere at a height of 400 km. The calculation is described by EVANS and TAYLOR (1961). In order to calculate $\int N . dh$ we used ionosonde data kindly provided by Mr H. J. A. VESSEUR of the Royal Dutch Meteorological Institute K.N.M.I. at De Bilt. For a parabolic F layer the value of this integral is $16.5 \times 10^{-9} (f_0F_2)^2 . y_mF_2$ electrons per cm², where f_0F_2 is the F layer critical frequency in c/s and y_mF_2 is the parabolic half-thickness in cm. We used the observed value of f_0F_2, interpolated where necessary, and the mean hourly values of y_mF_2 (averaged over the whole four weeks of observation, for each one-hour interval of MET separately). The internal mean error in the calculated Faraday rotation is probably of the order of 25%.

Figure 4 (p. 224) shows our results as correlation diagrams between θ_{gal} and the Faraday rotation expected for a parabolic F layer. As the error in θ_{gal} is inversely proportional to $\overline{T_b^p}$, we should expect any correlation to be lost amongst the errors for points with small $\overline{T_b^p}$. We expect this to happen for the point $l^{II} = 128°$, $b^{II} = +71°$, and do not consider the slight negative correlation significant. At the North pole the corrections were known more accurately, and the data may just be significant. The most reliable data are those for the other two points. The point $l^{II} = 141°$, $b^{II} = +8°$ was also observed in the daytime. These observations are confused by solar radiation in the sidelobes. We deduce this from the presence of large deviations in $\overline{T_b^p}$ from the nighttime value; if Faraday rotation were the sole disturbing factor, only angle variations would be found. If deviations in $\overline{T_b^p}$ from the nighttime value are small, the probability of a solar contribution is small and we have separated the data into two reliability classes accordingly. The greater spread in θ_{gal} for the less reliable class lends support to this procedure.

We conclude from Figure 4 that, wherever the data are reliable, there is evidence for ionospheric Faraday rotation. The slope of the lines representing the points is between 2 and 3, which agrees with earlier findings (e.g. EVANS and TAYLOR 1961) that the total electron content is larger than expected from a parabolic layer.

REFERENCES

J. V. EVANS and G. N. TAYLOR 1961, *Proc. Roy. Soc. A* **263**, 189.
GART WESTERHOUT, CH. L. SEEGER, W. N. BROUW and J. TINBERGEN 1962, *B.A.N.* **16**, 187 (No. 518).

FIGURE 4

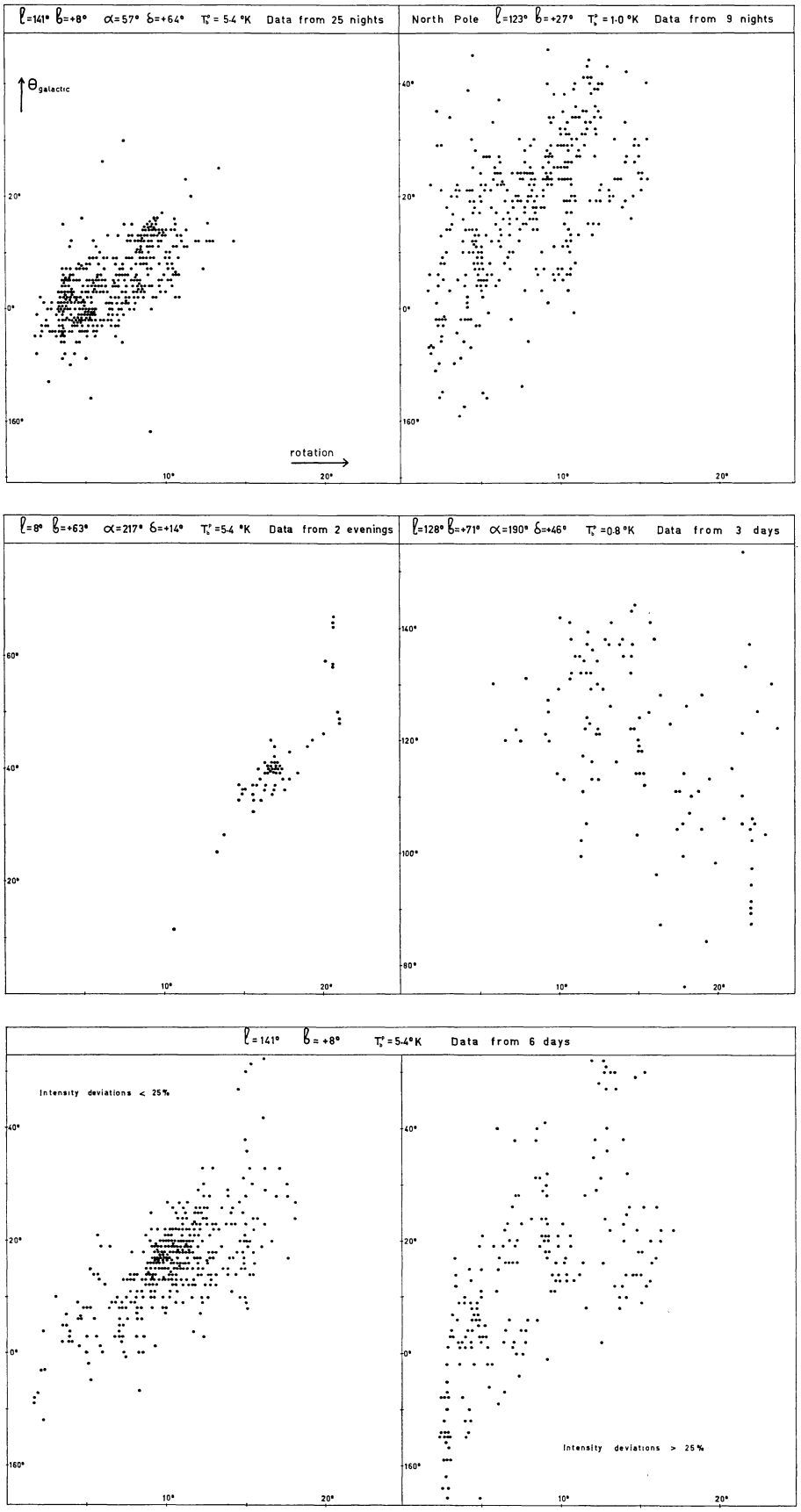

Correlation diagrams for θ_{gal} vs. Faraday rotation expected for a parabolic F layer. The values of T_b^p were derived from provisonal data.